RSC Advances

PAPER

View Article Online
View Journal | View Issue

Cite this: *RSC Adv.*, 2026, **16**, 19094

Nano-encapsulated *Senecio glaucus* L. essential oil with potent antioxidant, anticancer, and wound-healing properties

Zainab H. Hussein,[ab] Sherif F. Hammad,[cg] Kuniyoshi Shimizu,[d] Amr A. Nassrallah *[ae] and Hesham S. M. Soliman[fg]

Senecio glaucus L. essential oil (EO), rich in mono- and sesquiterpenes, demonstrates multiple bioactivities; however, it suffers from volatility and poor water solubility. This study developed a nano-encapsulation of EO to improve its stability and bioactivity. GC-MS analysis mainly identified terpene derivatives, with dehydrofukinone being the dominant compound (29.9%). Physical characterization confirmed the nano-sized structure of the essential oil-loaded nanoparticles (EO-NPs). Antioxidant assays (DPPH and ABTS) showed enhanced radical scavenging activity of EO-NPs with 14.07 ± 1.6 and 7.29 ± 1.33 μg mL^{-1} IC_{50} values, respectively. The MTT assay demonstrated notable *in vitro* anticancer effects of EO-NPs against PC3 prostate cancer (IC_{50} = 64.71 ± 2.91 μg mL^{-1}) and HCT-116 colorectal cancer cells (IC_{50} = 74.59 ± 2.3 μg mL^{-1}). At the molecular level, EO-NPs upregulated pro-apoptotic genes and proteins and downregulated anti-apoptotic Bcl-2. Additionally, EO-NPs exhibited promising wound healing activity in the migration scratch assay on BJ-1 fibroblast cells. These outcomes highlight the potential of EO-NPs as a therapeutic candidate with enhanced *in vitro* biological activity, warranting further investigation.

Received 17th December 2025
Accepted 10th March 2026

DOI: 10.1039/d5ra09763k

rsc.li/rsc-advances

1 Introduction

Essential oils (EOs), derived from plant sources, comprise various bioactive compounds, including terpenes, phenolics, and aliphatic hydrocarbons.[1,2] These compounds exhibit a range of biological activities, such as antimicrobial, antioxidant, and anticancer effects, and have wide applications in food, medicine, and cosmetics.[3–13] EOs also serve as preservatives and flavoring agents, as well as agricultural growth enhancers, herbicides, and insecticides.[14] Despite their promising potential, the practical use of EOs is limited by challenges such as high volatility, poor water solubility, and susceptibility to oxidation and degradation under environmental conditions.[15,16] Nanotechnology offers a promising approach to overcome these limitations. Nanoencapsulation of EOs can enhance their stability, bioavailability, and efficacy, while protecting them from oxidation and volatilization.[17–22] It also improves their solubility, reduces side effects, and allows for controlled release and targeted delivery to specific sites, thereby enhancing therapeutic outcomes.[15] Furthermore, encapsulating EOs in nanoparticles can facilitate their transport across biological barriers, extend circulation times, and improve their effectiveness and safety.[23,24] Natural polysaccharides, such as chitosan and hyaluronic acid, are increasingly explored as biopolymers for the nanoencapsulation of bioactive compounds like EOs.[25] These polymers offer numerous advantages, including high biocompatibility, biodegradability, and chemical modifiability. Chitosan, a cationic copolymer obtained from crustacean exoskeletons, has been extensively studied for applications in tissue engineering, drug delivery, and cosmetics due to its biocompatibility, mucoadhesiveness, and non-immunogenicity.[26] However, the cationic nature of chitosan can lead to rapid clearance and nonspecific interactions with serum proteins, potentially limiting its circulation time.[27] To overcome this limitation, chitosan nanoparticles can be surface-modified with anionic polysaccharides such as hyaluronic acid, which reduces protein adsorption and macrophage uptake. Hyaluronic acid, a naturally occurring glycosaminoglycan, exhibits excellent biocompatibility and bioadhesive properties. It plays a key role in biological processes such as wound healing, inflammation, and tissue regeneration and can target specific receptors such as CD44, which are overexpressed in certain cancer cells and inflammatory conditions.[28] Incorporating

[a]*Biotechnology Department, Faculty of Basic and Applied Sciences, Egypt-Japan University of Science and Technology, New Borg El-Arab, Alexandria, 21934, Egypt. E-mail: amr.nassrallah@ejust.edu.eg*
[b]*Department of Chemistry, Faculty of Science, Aswan University, Aswan 81528, Egypt*
[c]*Pharmaceutical Chemistry Department, Faculty of Pharmacy, Helwan University, Ain Helwan, Cairo 11795, Egypt*
[d]*Department of Agro-Environmental Sciences, Graduate School of Bioresource and Bioenvironmental Sciences, Kyushu University, Fukuoka 819-0395, Japan*
[e]*Biochemistry Department, Faculty of Agriculture, Cairo University, 12613 Giza, Egypt*
[f]*Department of Pharmacognosy, Faculty of Pharmacy, Helwan University, Ain Helwan, Cairo 11795, Egypt*
[g]*Faculty of Pharmacy, Egypt-Japan University of Science and Technology, New Borg El-Arab, Alexandria, 21934, Egypt*

hyaluronic acid into drug delivery systems enhances the targeting and selective uptake of therapeutic agents, particularly in oncology and wound healing applications. *Senecio glaucus* L. (SG), a member of the *Senecio* genus in the Asteraceae family, is an annual wildflower indigenous to regions of North Africa and parts of Asia. It is typically found in agrestal and ruderal sandy habitats, as well as on stony hillsides, rocky ground, and along riverbanks.[29] The essential oil of SG is mainly composed of monoterpenes, sesquiterpenes, and oxygenated terpenes.[30] Previous studies had demonstrated the biological significance of SG volatile compounds, including notable antimicrobial, antioxidant, and anticancer activities,[31] as well as antifungal, nematostatic, acaricidal, and repellent properties.[32]

Although extracts of SG have been employed in nanotechnology applications,[33–35] the essential oil from this plant has not yet been explored for nano-encapsulation development. Considering its established bioactivities, this represents a significant research gap. The chemical composition of EO suggests considerable potential for incorporation into nanoparticles and therapeutic applications. In the present study, we aim to develop a chitosan/hyaluronic acid CS–HA nanoencapsulated formulation of SG essential oil to improve its stability, bioactivity, and prospective therapeutic efficacy, particularly for wound healing and anticancer applications.

2 Materials and methods

2.1 Plant collection and identification

The aerial parts (leaves and stems) of SG were collected during the flowering season over a three-month period (February–April 2021) from the Aswan University campus, Aswan, Egypt. All samples were harvested from the same geographical location and at a consistent phenological stage to maintain compositional uniformity. The collected plant materials were pooled to form a single representative batch for the study. Botanical identification was performed at the Department of Botany, Faculty of Science, Aswan University, Egypt. The harvested samples were carefully cleaned, air-dried in the dark at room temperature, and finely ground into powder prior to essential oil extraction and further analysis.

2.2 Extraction of the volatile oil

The EO from the leaves and stems of SG was extracted by hydrodistillation using a standardized Clevenger-type apparatus.[36] Distillation was carried out for seven hours at 100 °C to ensure complete extraction of volatile components. The collected EO was dried over anhydrous sodium sulphate (Na_2SO_4) to remove residual moisture, then stored in airtight, light-resistant vials at low temperature to prevent oxidation and preserve stability prior to further analyses, such as GC-MS.

2.3 Chemical composition analysis of essential oil

The chemical composition of the volatile oils was analyzed using gas chromatography (GC) coupled with an Ultra Shimadzu QP 2010 mass spectrometer, equipped with a TRB-WAX capillary column (30 m × 0.25 mm i.d., 0.25 μm film thickness). Purified helium was used as the carrier gas at a constant flow rate of 1.0 mL min^{-1}. A split ratio of 1 : 150 was applied. The oven temperature program started with an initial hold at 60 °C for 3 min, followed by a gradual increase at 5 °C min^{-1} to 260 °C, which was maintained for 15 min. The injection temperature was 260 °C, and a 1 μL sample (diluted 10 : 100 in pure hexane) was injected. Mass spectra were acquired in electron ionization (EI) mode with an ionization energy of 70 eV, scanning a mass-to-charge (m/z) range of 10–400. Compound identification was performed using a dual approach: (1) comparison of retention indices (RI) calculated against a homologous *n*-alkane series (C7–C30) and (2) library matching using the NIST 11 Mass Spectral Library.

2.4 Preparation of the EO hyaluronic acid functionalized chitosan nanoparticles

An ionic gelation technique, based on Chiesa *et al.*,[37] was employed with slight modifications. The CS–HA nanoencapsulation was chosen due to the complementary physicochemical and biological properties of its components, making it suitable for essential oil encapsulation. Chitosan (CS), under mildly acidic conditions (pH 5), carries a positive charge that enables electrostatic interaction with polyanionic crosslinkers, facilitating stable nanoparticle formation *via* ionic gelation. Hyaluronic acid (HA) was incorporated to improve nanoparticle stability, enhance hydrophilicity, and provide potential biological targeting due to its affinity for CD44 receptors, which are often overexpressed in cancer cells. Tripolyphosphate (TPP) was added to reinforce ionic crosslinking and enhance structural integrity. The polymer concentrations and oil-to-polymer ratio were based on a previously optimized formulation and confirmed through preliminary trials to yield reproducible nano-sized particles with good dispersion stability and encapsulation efficiency. Alternative concentrations were tested, but the reported composition provided the most consistent physicochemical properties and biological compatibility. For nanoparticle preparation, a 4 mg mL^{-1} chitosan solution was dissolved in 1% (w/v) aqueous acetic acid, stirred at room temperature, and kept overnight under mild stirring. The solution was filtered through a 0.45 μm Millipore filter, and Tween 80 (0.1 mg mL^{-1}) was added. The pH was adjusted to 5 using 0.1 M NaOH. The essential oil was dispersed in 0.5 mL of ethanol and added to the chitosan/Tween 80 solution under continuous stirring. The ratio of essential oil to chitosan was 0.5 : 1 w/w. Hyaluronic acid (10 mg mL^{-1}) and TPP (0.5 mg mL^{-1}) were separately dissolved in distilled water and mixed at a 4 : 1 v/v ratio. This mixture was filtered through a 0.45 μm Millipore filter. In acidic conditions, chitosan amino groups are positively charged, facilitating interactions with the polyanionic crosslinkers. The carboxyl and hydroxyl groups of HA further contribute to crosslinking and hybrid system formation. The chitosan/oil dispersion was added dropwise to an equal volume of the HA/TPP mixture using a 23-gauge syringe while stirring at 1000 rpm. Nanoparticles spontaneously formed and crosslinked. The mixture was stirred continuously for 15 min at room temperature. Nanovesicles were collected by centrifugation

at 7000 rpm for 60 min at 4 °C and retained for further characterization.

2.5 Evaluation of entrapment efficiency percentage (EE%) in the prepared oil nano-encapsulation

The entrapment efficiency (EE%) of the hyaluronic acid–chitosan nanoparticles (NPs-Cont) was quantitatively determined indirectly by quantifying the unentrapped EO in the separated supernatant.[38,39] Following centrifugation at 7000 rpm for 30 minutes at 4 °C, the supernatant was collected and filtered through a 0.2 μm Millipore membrane filter. The filtered supernatant was then diluted with ethanol and analyzed spectrophotometrically at 252 nm using a standard calibration curve.

The EE% was measured using the following equation:

$$\mathrm{EE\%} = \frac{\text{mass of EO added} - \text{mass of free EO in the supernatant}}{\text{mass of EO added}} \times 100$$

2.6 Characterization of the prepared nano-encapsulation

2.6.1 Size (PS), polydispersity index (PDI), and zeta potential (ZP) analysis. The particle size (PS), polydispersity index (PDI), and zeta potential (ZP) of the prepared oil formulations were assessed using a Zeta Sizer (Malvern Instruments Ltd, Nano Series ZS90, IUK). The measurements were carried out at 25 °C using a helium–neon laser operating at 632 nm and a detection angle of 90°. The Zeta Sizer is capable of measuring ZP values within the range of −120 to +120 mV. Prior to analysis, the samples were subjected to dilution at a 1 : 20 (v/v) ratio with deionized water to ensure optimal measurement conditions. Each formulation, to ensure the accuracy and reproducibility of the results, was analyzed in triplicate.

2.6.2 Transmission electron microscopy (TEM) analysis. Morphological properties of the nanoparticles were measured using a transmission electron microscopy (TEM) using a JEOL JEM-2100 microscope (JEOL CO., JAPAN). The nanoparticle suspension was carefully diluted at a 1 : 20 (v/v) ratio in bi-distilled water. A drop of the diluted sample was placed on a carbon-coated copper grid, then stained with 2% phosphotungstic acid to enhance contrast. The grid was allowed to air-dry before being analyzed under the TEM.

2.6.3 Fourier transform infrared (FT-IR) spectroscopic analysis. FT-IR analysis was performed to confirm nanoparticle formation and identify potential molecular interactions between components. The EO, EO-NPs, NPs-Cont physical mixture, and optimized formulation were analyzed using a PerkinElmer spectrophotometer (Waltham, MA, USA) with the KBr pellet method. Samples were mixed with spectroscopic-grade anhydrous potassium bromide (KBr) and compressed under vacuum to form transparent pellets of uniform thickness. Spectra were recorded over the mid-infrared range (400–4000 cm^{-1}) at a resolution of 4 cm^{-1}, with 32 scans per sample to ensure signal accuracy. This analysis enabled the identification of functional groups and molecular interactions within the samples. FT-IR spectra of all samples were compared to detect shifts in characteristic absorption peaks, indicating chemical bonding changes or encapsulation of the essential oil.

2.7 Biological assessments

2.7.1 Antioxidant activity. The antioxidant scavenging potential of EO, EO-NPs, and NPs-Cont was assessed using both ABTS and DPPH assays.

2.7.1.1 DPPH assay. The free radical scavenging capacity of the samples was quantitatively evaluated using (DPPH) assay described by Li *et al.*, with minor modifications.[40] Briefly, 900 μL of 50 mM DPPH solution was added to 100 μL of diluted test samples at varying concentrations, vortexed, and incubated in the dark at room temperature for 30 minutes. Ascorbic acid and methanol were used as positive and negative controls, respectively.

2.7.1.2 ABTS assay. ABTS radical scavenging activity was measured using a method adapted from Re *et al.*, with slight modifications.[41] ABTS solution (7 mM) was mixed with an equal volume of 2.45 mM potassium persulfate and incubated at 4 °C in the dark for 16 hours. The absorbance of the ABTS reagent was adjusted to 0.7 ± 0.03 at 734 nm. Subsequently, 900 μL of ABTS reagent was mixed with 100 μL of the tested sample, incubated in the dark at room temperature for 15 minutes, and the absorbance was measured at 734 nm.

2.7.1.2.1 Calculation of radical scavenging activity. For both assays, the percentage inhibition of free radicals was calculated using a single standardized equation:

$$\text{Inhibition (\%)} = (A_0 - A_s)/A_0 \times 100$$

where A_0 is the absorbance of the control (reaction mixture without sample), and A_s is the absorbance of the tested sample.

Both assays were performed in triplicate to evaluate the radical scavenging activity of EO, EO-NPs, and NPs-Cont.

2.7.2 MTT assay. The cytotoxic effects of (EO, EO-NPs, NPs-Cont) were evaluated against HCT-116 (ATCC® CCL-247™), HepG-2 (ATCC® HB-8065™), MCF-7 (ATCC® HTB-22™), PC3 (ATCC® CRL-1435™), and RPE-1 (ATCC® CRL-4000™) cells using the MTT assay with slight modifications.[42] Cells were seeded in 96-well plates at 1×10^4 cells per well and incubated for 24 h to allow attachment. Subsequently, cells were treated in triplicate with EO, EO-NPs, and NPs-Cont at 12.5, 25, 50, and 100 μg mL^{-1} for 48 h.

After treatment, 40 μL of MTT solution (2.5 mg mL^{-1} in PBS) was added to each well and incubated for 3 h at 37 °C. Formazan crystals formed by viable cells were dissolved with 100 μL of 10% SDS solution and incubated overnight. Absorbance was measured at 570 nm using a microplate reader. Cell viability was calculated relative to untreated controls, and IC_{50} values were derived from dose–response curves using nonlinear regression analysis.

2.7.3 Gene expression profiling. mRNA transcripts of essential pro- and anti-apoptotic marker genes were analyzed within PC3, HCT-116, HepG-2, and RPE-1 cells exposed to IC_{50} concentrations for 72 h. RNA was extracted using the Total RNA

Purification Kit (Norgen Biotek Corp., Thorold, ON, Canada) as the manufacturer's instructions stated. RNA quality was assessed and subjected to cDNA synthesis as previously described.[43] Amplification programs and PCR amplicon specificity were carried out with Rotor-Gene 6000 (Corbett Life Sciences, Sydney, Australia) in 100-well Gene Discs with QuantiTect SYBR-Green PCR Kit (Qiagen, Germany) as previously documented in standard protocols.[44] Gene expression analysis and PCR thermal cycling program to measure the fold change relative to the 18S gene were performed as previously reported.[45]

2.7.4 Scratch wound healing test. The scratch assay was carried out using the scratch technique according to previously reported methods.[46,47] In brief, fibroblast human normal cell line BJ-1 (ATCC® CRL-2522™) was plated into 12-well cell culture plates at 37 °C, 5% CO_2 with a concentration of 2×10^5 cells per well in a medium containing 10% FBS. After incubation for 24 h, the cell monolayers were scraped linearly using a sterile yellow micropipette tip to create a scratch, and the wells were then washed to remove detached cells. Cells were subsequently treated for 24 h with either EO, EO-NPs, and NPs-Cont as a control. The applied concentration for EO and EO-NPs was 50 μg mL^{-1}. Untreated cells served as a negative control. Images were captured using a digital camera mounted on an inverted microscope and analyzed to assess cell migration and morphological changes.

2.7.5 Statistical analysis. GraphPad Prism 9 software (version 9.1.0 (221), La Jolla, CA, USA) was used for statistics, and the data were evaluated using 2-way ANOVA with the recommended Tukey's multiple comparisons test. The results were reported as mean ± SD ($n = 3$). Significance was accepted at $P < 0.05$.

3 Results and discussion

3.1 GC-MS characterization of the chemical composition of EO

In the present study, the essential oil extracted from the leaves and stems of SG yielded 0.5%, appearing as a transparent yellow oil with a clear appearance. Gas chromatography analysis and chemical identification by GC-MS were performed. In Fig. 1, the total ion chromatogram (TIC) exhibited several peaks that mainly belonged to terpenes and hydrocarbons, which were identified according to the NIST11 library and comparison of their retention indices with those reported in the literature. Among the detected peaks, the chromatogram showed a distinct peak at a retention time of 32.23 minutes, which was the most abundant component (48.88% of the total area), corresponding to dehydrofukinone with a molecular weight of 218 and significant fragmentation peaks at m/z 161 and 147. The predominance of dehydrofukinone strongly influences the biological profile of EO. As a sesquiterpene ketone, dehydrofukinone possesses moderate lipophilicity, enabling efficient interaction with biological membranes, which may underlie its reported antifungal, sedative, anaesthetic, and anticonvulsant properties.[48,49] Its high abundance suggests that it is a principal contributor to the observed bioactivities of the oil, either directly through membrane disruption and modulation of cellular signaling pathways, or indirectly through synergistic interactions with co-occurring terpenoids.

The occurrence of dehydrofukinone in different segments of several *Senecio* genera has been established by previous studies.[50–54] It was previously reported from SG and identified as a major component (21%) of its essential oil by De Pooter and colleagues, who confirmed its structure using IR, UV, and 1D-NMR spectroscopy after preparative GC isolation.[30] Furthermore, with respective amounts of 17.20% and 19.90%, dehydrofukinone was identified as the third most prevalent constituent in essential oils extracted from SG capitula and shoots.[31] A recent study on volatile oils extracted from the whole plant of SG reported dehydrofukinone as a major sesquiterpene constituent (27.15%); the compound was subsequently isolated *via* HPLC and structurally elucidated using ^{1}H- and ^{13}C-NMR spectroscopy.[55] These findings from different Egyptian regions—the Cairo-Ismailia desert road,[30] the Egyptian eastern desert,[31] and the Nile Delta,[55] confirm that dehydrofukinone is consistently a key volatile marker of the species. Other notable terpenoid compounds were detected (Table 1), including the monoterpene α-terpineol (0.53%), the diterpenoid phytol (3.18%), and the sesquiterpenes valencene (3.05%), curcumene (2.75%), caryophyllene oxide (0.6%), α-humulene (0.58%), and α-selinene (0.56%). These constituents, although present in lower proportions, may significantly modulate the overall biological response. EOs are known to exert bioactivity through multi-target mechanisms, including membrane permeabilization, enzyme inhibition, oxidative stress modulation, and interference with quorum sensing in microorganisms.

Importantly, the overall essential oil often demonstrates greater biological efficacy than its isolated constituents, indicating synergistic interactions.[58] Mechanistically, synergy may arise when one component enhances membrane permeability, facilitating the intracellular penetration of other active compounds, or when multiple constituents target complementary biochemical pathways, resulting in amplified biological responses.

From an encapsulation perspective, the high content of dehydrofukinone and the presence of volatile terpenoids make EO particularly suitable for nanoencapsulation. Due to their hydrophobicity, volatility, and susceptibility to oxidative degradation, terpenoid-rich oils may suffer from instability and limited aqueous solubility. Nanoencapsulation systems can enhance physicochemical stability by protecting active constituents from evaporation, oxidation, and photodegradation. Moreover, nanoscale carriers enable improved dispersion in aqueous media, increased surface area, enhanced membrane interaction, and controlled release kinetics. Crucially, nanoencapsulation may also preserve and enhance synergistic interactions among oil components. By co-encapsulating multiple terpenoids within the same nanocarrier, their relative proportions can be maintained during delivery, preventing preferential loss of more volatile constituents. Controlled and sustained release ensures simultaneous availability of active compounds at the target site, thereby supporting cooperative biological effects. Enhanced cellular uptake of nanodroplets further promotes effective interaction with microbial or

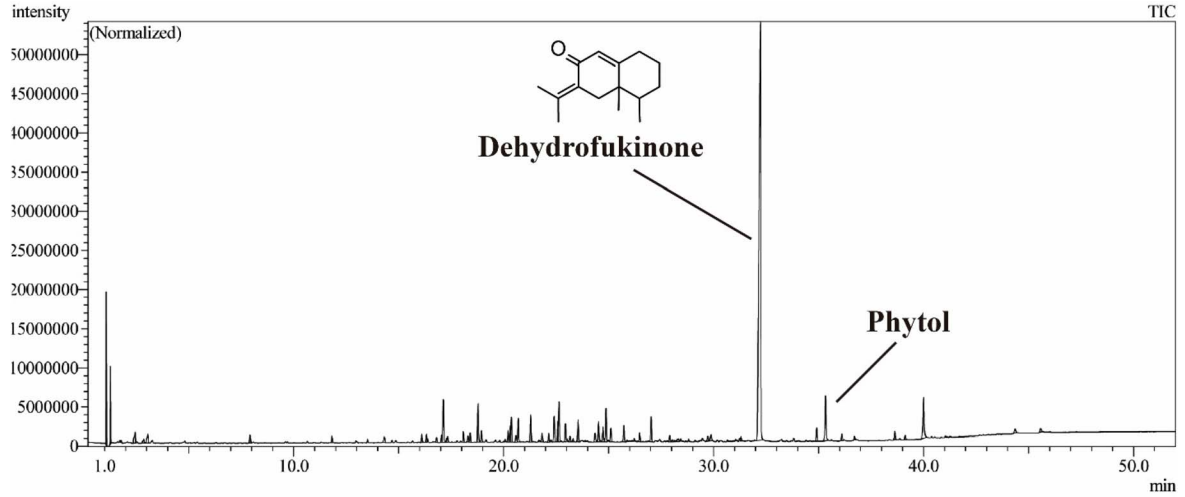

Fig. 1 Total ion chromatogram (TIC) of EO analyzed by GC-MS, highlighting a major peak corresponding to dehydrofukinone and phytol at 32.23 and 35.33 minutes, respectively.

mammalian cell membranes, potentially amplifying the intrinsic bioactivity of dehydrofukinone-rich oils.

The chromatographic profile (Fig. 1) thus illustrates a chemically complex EO dominated by dehydrofukinone and supported by a diverse array of minor terpenoids. This compositional profile not only explains the biological potential of EO but also provides a strong rationale for nano-encapsulation as a strategy to optimize stability, delivery efficiency, and synergistic therapeutic performance.

3.2 Preparation of the nano-encapsulation

Ionic gelation is a widely favored technique used for the synthesis of SH-NPs. It facilitates the simple encapsulation of sensitive molecules under mild conditions without requiring harsh organic solvents or high temperatures, which may damage sensitive molecules. This procedure is safe since it does not use harsh organic solvents or elevated temperatures that could compromise bioactive compounds. Ionic gelation is often used to encapsulate active compounds, including EOs, for application in food, cosmetics, and pharmaceutical products. Importantly, two conceptually distinct processes occur during nanoparticle preparation: (i) electrostatic crosslinking and (ii) surface functionalization. It relies on the ionic interactions and crosslinking between the negatively charged polyanionic components, such as sodium tripolyphosphate (TPP), and the positively charged chitosan chains. The primary electrostatic crosslinking mechanism occurs between chitosan and TPP, where the negatively charged phosphate groups of TPP interact with the protonated amino groups of chitosan, forming a three-dimensional ionically crosslinked network responsible for nanoparticle formation and structural stabilization.

In contrast, hyaluronic acid (HA) deposition represents a surface functionalization process rather than a primary crosslinking step. While HA is also negatively charged and can interact electrostatically with chitosan, its role is mainly to modify the nanoparticle surface through polyelectrolyte complexation with residual positively charged amino groups exposed on the nanoparticle interface.

The conventional multistep procedure involves the addition of polyanionic sodium tripolyphosphate, followed by the addition of hyaluronic acid. This method can produce chitosan–hyaluronic acid nanoparticles with a neutral or positive surface charge. Such surface charge profiles indicate partial or limited HA surface coverage, as complete surface functionalization

Table 1 Major terpenoid constituents of EO as identified by GC-MS[a]

No.	Compound	RT	Area%	Height%	Mwt	MF	RI_{dtm}	RI_{lit}
1	Dehydrofukinone	32.23	48.88	29.9	218	$C_{15}H_{22}O$	1678	1678 (ref. 31 and 52), 1688 (ref. 56)
2	Phytol	35.33	2.86	3.18	296	$C_{20}H_{40}O$	2045	2045 (ref. 31), 2058 (ref. 56), 2099 (ref. 57)
3	Valencene	17.12	2.46	3.05	204	$C_{15}H_{24}$	1474	1471 (ref. 31), 1488 (ref. 56)
4	Curcumene	18.78	2.20	2.75	202	$C_{15}H_{22}$	1524	1479 (ref. 56 and 57)
5	Caryophyllene oxide	24.35	0.57	0.60	220	$C_{15}H_{24}O$	1507	1582 (ref. 56)
6	α-Humulene	16.101	0.49	0.58	204	$C_{15}H_{24}$	1579	1449 (ref. 57), 1452 (ref. 56)
7	α-Selinene	16.32	0.52	0.56	204	$C_{15}H_{24}$	1502	1498 (ref. 56)
8	α-Terpineol	17.050	0.44	0.53	154	$C_{10}H_{18}O$	1143	1186 (ref. 56)

[a] RI_{dtm} = the determined retention indices, RI_{lit} = the reference retention indices from literature.

would be expected to significantly reduce or reverse the positive zeta potential of chitosan nanoparticles.

Therefore, HA surface deposition should not be assumed but rather inferred from physicochemical characterization. A shift in zeta potential toward less positive or more negative values suggests masking of surface amino groups by HA. Additionally, FT-IR spectra showing characteristic HA carboxylate ($-COO^-$) absorption bands at the nanoparticle surface further support HA surface localization.

On the other hand, the adopted method in this study is based on the Chiesa *et al.*, 2018 technique, with slight modification.[37] It is a one-step process to produce hyaluronic-functionalized chitosan nanoparticles with enhanced HA surface exposure, allowing for more precise targeting and cellular internalization. In this modified method, which is described as inverse ionic gelation, a fixed volume of chitosan solution is added to a similar volume of an aqueous solution mixture containing both hyaluronic acid and TPP.

In this inverse ionic gelation approach, nanoparticle formation (chitosan–TPP crosslinking) and HA interfacial complexation occur simultaneously, favoring greater availability of HA at the particle surface compared to the conventional sequential method.

Surface-exposed HA plays a critical biological role due to its high affinity for CD44 receptors, which are overexpressed in many cancer cells and are involved in cell adhesion, migration, and proliferation. HA-decorated nanoparticles can bind to CD44 receptors and undergo receptor-mediated endocytosis, thereby enhancing selective cellular uptake in CD44-overexpressing tumor cells. In the context of wound healing, HA–CD44 interactions promote keratinocyte and fibroblast migration, regulate extracellular matrix remodeling, and modulate inflammatory responses. Consequently, improved HA surface exposure may enhance cellular targeting, tissue regeneration, and therapeutic efficacy in both anticancer and regenerative applications.

3.2.1 Evaluation of encapsulation efficiency (EE%) of EO-loaded chitosan–hyaluronic acid nanoparticles. The encapsulation efficiency (EE%) of the formulated chitosan–hyaluronic acid functionalized nanoparticles (NPs-Cont) loaded with EO was determined to be 71.3 ± 8.2%. This high efficiency can be attributed to the strong polycationic–polyanionic interactions between the polymeric components and the role of tripolyphosphate (TPP) in enhancing cross-linking. These interactions promote the formation of a dense and stable encapsulating matrix, aided by the abundance of functional groups available for ionic bonding and cross-linking. The resulting nanoparticles are compact and robust, which minimizes oil leakage and improves entrapment stability.

However, encapsulation of EOs cannot be explained by electrostatic interactions alone, as EOs are predominantly hydrophobic in nature. Their limited aqueous solubility promotes preferential partitioning into the hydrophobic domains of the polymeric matrix during nanoparticle formation. This hydrophobic partitioning plays a crucial role in retaining the oil within the interior of the nanoparticles.

Furthermore, the presence of hydroxyl and amine groups in chitosan, as well as hydroxyl groups in phenolic compounds of the EO, enables the formation of hydrogen bonds and electrostatic interactions. These molecular interactions further contribute to the high encapsulation efficiency by strengthening the association between the EO and the polymeric matrix.

Therefore, the observed EE% is likely the result of multiple complementary mechanisms, including: (i) ionic crosslinking between chitosan and TPP, which creates a compact three-dimensional network; (ii) hydrophobic partitioning of essential oil constituents into the less polar regions of the polymer matrix; and (iii) matrix densification induced by crosslinking, which reduces porosity and limits diffusion-driven oil leakage. The combined effect of these structural and physicochemical interactions explains the relatively high and stable encapsulation efficiency observed in this system, rather than electrostatic forces alone.

3.2.2 Nanoparticle characteristics: polydispersity index, particle size, and zeta potential. The measured hydrodynamic particle size was 333.6 ± 85 nm. The nanosized particle size indicates the effectiveness of the preparation procedure. Although this size falls within the nanoscale range (<1000 nm), it is relatively large compared to smaller nanocarriers (<200 nm), and this may influence cellular uptake behavior and biological performance. Particles in the 300 nm range are more likely to be internalized *via* mechanisms such as macropinocytosis or caveolae-mediated pathways rather than exclusively clathrin-mediated endocytosis. Additionally, this size may affect tissue penetration, biodistribution, and retention time, which should be considered when interpreting biological outcomes.

Also, the polydispersity index (PDI) value was 0.342. The results demonstrated that the formulated particles had a nanoscale size distribution with moderate and acceptable homogeneity rather than high uniformity. A PDI value that is less than 0.5 indicates that the particle size of the measured sample has a reasonably narrow and acceptable distribution, although values below 0.3 are typically considered highly monodisperse.

Moreover, the zeta potential of the formulation was −33.2 ± 4.9 mV. This value reflects the successful functionalization of chitosan nanoparticles with hyaluronic acid. The localization of hyaluronic acid on the outer surface of the NPs neutralizes the positive charge of chitosan and imparts a moderately negative zeta potential. This surface charge modification enhances electrostatic repulsion between particles, thereby preventing aggregation and ensuring sufficient colloidal stability of the formulated nanoparticles. Furthermore, a negative surface charge may reduce non-specific protein adsorption (opsonization) under physiological conditions, potentially improving dispersion stability in biological fluids and enhancing *in vitro* and *in vivo* performance.

3.2.3 Analysis of transmission electron microscopy (TEM). The morphological characteristics of the nanoparticles, as shown in Fig. 2, demonstrate a well-defined, spherical, and unaggregated structure. The EO-NPs exhibit a darker central core surrounded by a faint, lighter grey outer shell, indicating the presence of a surface coating likely corresponding to the

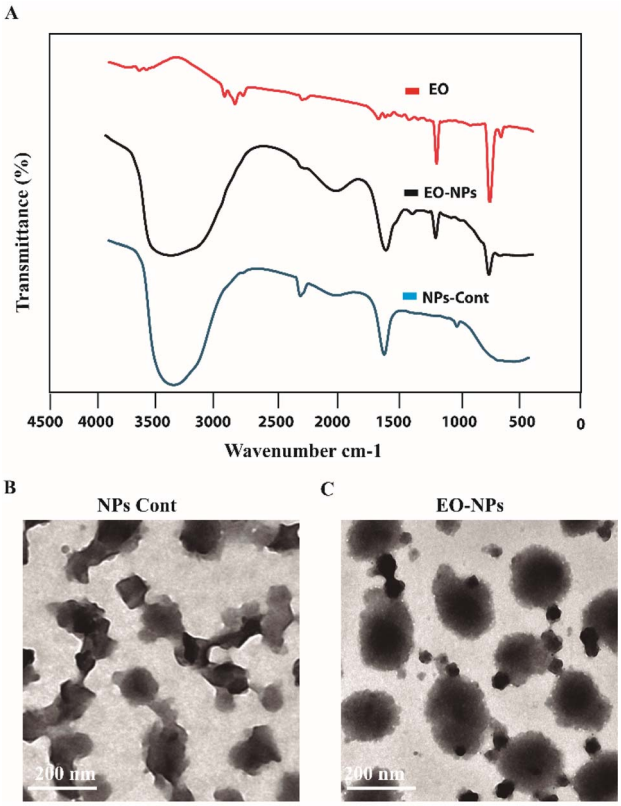

Fig. 2 Physical characterization of formulated nano-essential oil. (A) FT-IR analysis for EO, EO-NPs, and NPs-Cont. (B) TEM image for the NPs-Cont, (C) TEM image for the EO-NPs.

nanoparticle matrix or functionalizing agents. This coating further supports successful encapsulation. The particles appear uniform in size, and their dimensions are consistent with the average particle size obtained from dynamic light scattering (DLS) analysis, confirming the nanoscale range and good dispersion without significant aggregation.

3.2.4 FT-IR measurements. FT-IR analysis was performed to provide crucial information about the possible interactions involved in the nanoformulation process. The formation of the nanoformulation was evaluated based on shifts, appearance, or changes in intensity of characteristic peaks in the FT-IR spectra, indicating physical entrapment and non-covalent interactions rather than inclusion complex formation. As shown in Fig. 2, the FT-IR spectra of the EO, EO-NPs, and NPs-Cont are presented for comparison.

The EO spectrum displayed characteristic peaks at 761 cm^{-1} and 1219 cm^{-1} (Table 2), corresponding to C–H bending vibrations and C–O stretching, respectively. These peaks are characteristic of the essential oil's molecular structure and functional groups. The FTIR spectrum of the NPs-Cont revealed prominent peaks at 3442 cm^{-1}, assigned to –OH stretching vibrations, indicating the presence of hydroxyl groups. Additionally, a strong peak at 1637 cm^{-1} was observed, corresponding to C=C–O stretching, typically associated with the polymeric or organic structure of the nanoparticle matrix.

Interestingly, the EO-NPs spectrum showed a combination of characteristic peaks from both the EO and the NPs-Cont. The retention of key peaks from both components in the EO-NPs spectrum, despite slight shifts and changes in intensity, strongly suggests that interactions occurred between the essential oil molecules and the nanoparticle carrier. Importantly, the absence of new characteristic peaks or significant peak disappearance indicates that no covalent chemical modification occurred during nanoparticle formation. Instead, the encapsulation process is governed by physical entrapment within the ionically crosslinked chitosan matrix and non-covalent interactions such as hydrogen bonding and electrostatic forces.

Previous research has shown that the stabilization of nanoformulation systems depends critically on electrostatic interactions, which include both attractive and repulsive forces between charged molecules. By reducing the possibility of precipitation (where solid particles form and settle out) or phase separation (where components split into multiple layers), these forces aid in maintaining the formulation's structural integrity.[59] These interactions are indicative of successful encapsulation of the essential oil within the nanoparticle structure, forming a stable nanoformulation.

The preservation of the essential oil's characteristic functional group signals further confirms that its chemical structure remained intact after encapsulation. This represents a key advantage of the ionic gelation method, as maintaining structural integrity is essential for preserving the intrinsic biological activity of the essential oil. This encapsulation strategy is crucial for enhancing stability, solubility, and controlling the release properties of the essential oil when formulated into nanoparticles. Thus, the FT-IR analysis confirms the successful formation of essential oil-loaded nanoparticles through physical entrapment and non-covalent interactions, supporting the structural preservation of the essential oil after incorporation and suggesting that the developed system can offer promising stability and bioavailability improvements.

3.3 Biological assessments

3.3.1 Antioxidant capacity. Despite the antioxidant capability of synthetic antioxidants, their toxicity and adverse effects have prompted increasing interest in natural antioxidants being incorporated into food and medical products, which directly impact human health.[60] The inhibitory activity of the examined

Table 2 Characteristic FT-IR peaks and functional group assignments of studied samples

Sample	Key FTIR peaks (cm^{-1})	Assignment
EO	761, 1219	C–H bending, C–O stretch
NPs-Cont	3442, 1637	–OH stretch, C=C–O stretch
EO-NPs	Mixed (EO + NPs-Cont) peaks	Combination of EO and matrix

samples against DPPH and ABTS radicals, as represented in Fig. 3. Both tests provided a more complete overview of the antioxidant characteristics and strengthened the reliability of the data, as they use different types of radicals, solvents, and reaction kinetics. In general, the nano-encapsulation of EO displayed significant antioxidant activity, as determined by both assays, compared to the EO. The results also revealed that antioxidant activity increased in response to higher concentrations. The concentration required to achieve 50% inhibition (IC_{50}) is presented in Table 3. The results reflect the success of the chitosan-functionalized hyaluronic acid NPs in protecting the entrapped EO active components and maintaining their antioxidant activity, particularly phenolics and terpenes.[61,62] Importantly, the enhanced antioxidant activity of EO-NPs cannot be attributed solely to increased surface area. Nano-encapsulation also protects labile terpenoid and phenolic constituents from oxidative degradation, evaporation, and environmental exposure, thereby preserving their radical-scavenging capacity and improving functional stability over time. In addition, the EO-NPs exhibited improved antioxidant activity partly owing to their increased dispersion and surface accessibility compared to the free oil.[63–66] However, the essential oil constituents remain the primary contributors to radical scavenging activity, while chitosan and hyaluronic acid play a supportive role. The distinctive antioxidant capacity demonstrated by the investigated EO-NPs can be partially credited to the presence of functional groups in chitosan and hyaluronic acid that may facilitate hydrogen or electron donation. Nevertheless, the relatively high IC_{50} values of NPs-Cont compared to EO and EO-NPs clearly indicate that the polymers alone contribute modestly and synergistically rather than dominantly to the overall antioxidant effect. Different studies have reported that chitosan can enhance the antioxidant performance of entrapped active components,[67–70] while hyaluronic acid has been shown to augment DPPH radical scavenging of incorporated bioactive agents.[71–73] Thus, their role in the present system is best described as stabilizing and synergistic, enhancing the functional performance of the encapsulated essential oil rather than acting as primary antioxidants. As shown in Table 3, although ascorbic acid exhibited lower IC_{50} values in both assays, the developed nano-encapsulation is not intended to replace pure antioxidant standards such as ascorbic acid. Instead, it represents a multifunctional natural delivery system that combines antioxidant activity with improved stability, controlled release, and potential targeting or regenerative properties.

Table 3 Comparative IC_{50} results of EO and its nano formula

Material	IC_{50} (μg mL^{-1}) in DPPH	IC_{50} (μg mL^{-1}) in ABTS
EO	21.36 ± 1.9	9.43 ± 0.96
EO-NPs	14.07 ± 1.6	7.29 ± 1.33
NPs-Cont	69.18 ± 8.7	21.89 ± 8.4
Ascorbic acid	6.34 ± 0.08	4.08 ± 0.11

Therefore, the prepared EO chitosan-functionalized hyaluronic acid NPs present a promising, completely natural (green) nano-encapsulation with augmented and stabilized antioxidant activity, suitable for applications in food additives, biomedical formulations, or topical cosmeceutical systems aimed at combating oxidative stress-related disorders and supporting tissue regeneration.

3.3.2 Cytotoxicity evaluation. The development of nano-encapsulated EOs has gained significant interest as a strategy to boost their anticancer activity.[74] In our study, the *in vitro* cytotoxic activity of the three tested samples against four cancerous cell lines, HCT-116, HepG-2, MCF-7, and PC3, is shown in Fig. 4. The EO-NPs exhibited more effective cytotoxic properties, with IC_{50} values reported in Table 4, in comparison to EO and NPs-Cont, with the exception of MCF-7, where reduced cytotoxicity reflects the cell-line-dependent behavior rather than being unpredictable. Previous studies have reported that essential oil nano-encapsulations often exhibit enhanced cytotoxic effects compared to free oils.[75–81] However, opposite

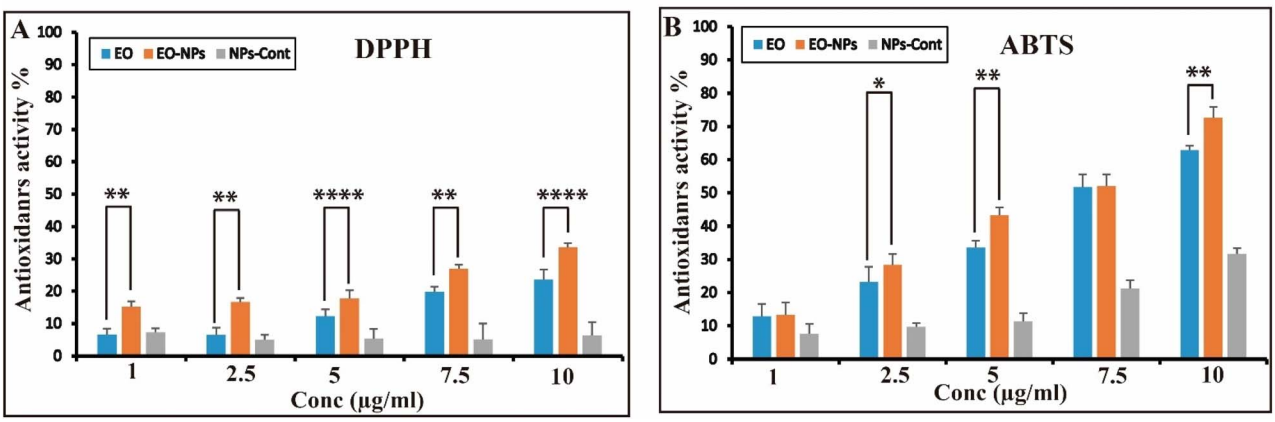

Fig. 3 (A) DPPH and (B) ABTS scavenging activity of the EO, EO-NPs, and NPs-Cont. The mean ± standard deviation (SD) of three triplicate determinations is used to express the results. Tukey's multiple comparisons test was used in conjunction with two-way ANOVA for statistical analysis. *$P < 0.05$, **$P < 0.01$, ***$P < 0.001$, and ****$P < 0.0001$ were established as significance thresholds for comparison differences between experimental samples.

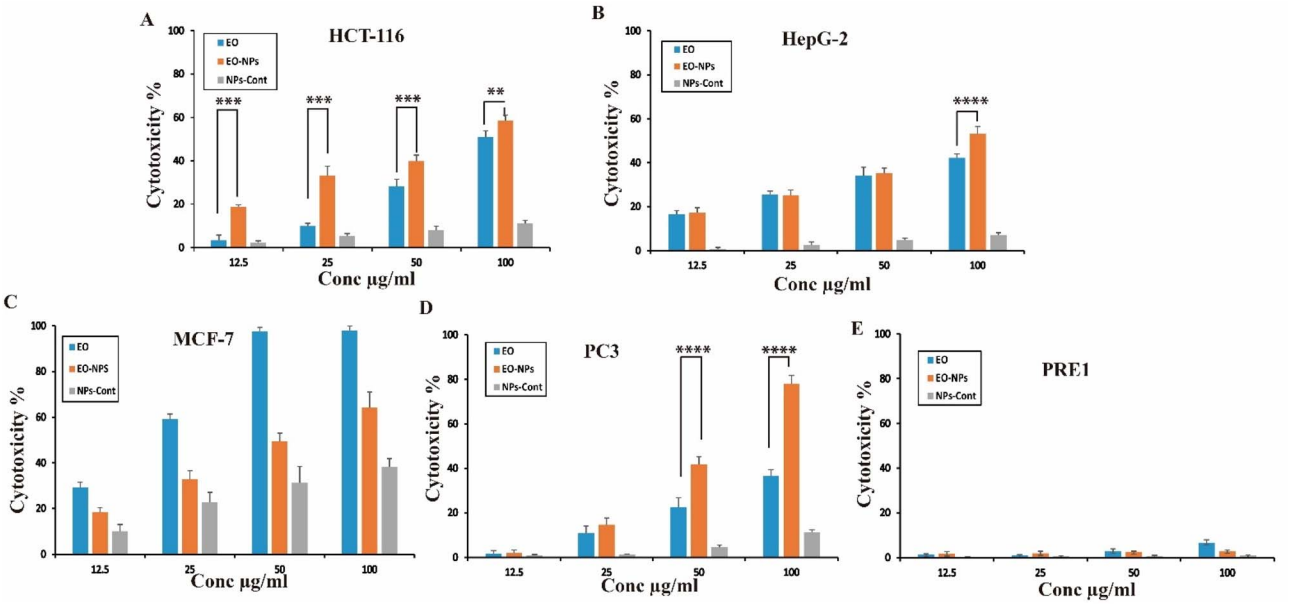

Fig. 4 Cytotoxicity results of EO, EO-NPs, and NPs-Cont against (A) HCT-116, (B) HepG-2, (C) MCF-7, (D) PC3, (E) RPE1. The mean ± standard deviation (SD) of three triplicate determinations is used to express the results. Tukey's multiple comparisons test was used in conjunction with two-way ANOVA for statistical analysis. *P < 0.05, **P < 0.01, ***P < 0.001, and ****P < 0.0001 were established as significance thresholds for comparison differences between experimental samples.

Table 4 IC_{50} data of the EO, EO-NPs and NPs-Cont cytotoxicity effect

	IC_{50} (µg mL^{-1})		
Cell line	EO	EO-NPs	NPs-Cont
HCT-116	97.75 ± 1.3	74.59 ± 2.3	404.85 ± 62.67
HepG-2	98.18 ± 3.4	83.84 ± 2.5	641 ± 94.6
MCF-7	40.22 ± 0.6	66.97 ± 4.36	110.42 ± 14.75
PC3	130.67 ± 4.35	64.71 ± 2.91	479.7 ± 52.79
RPE1	777.7 ± 105	1363 ± 265	4358 ± 1041

observations, where free EOs show greater activity than nano-encapsulated forms, have also been documented, such as in the case of free ginger EO toward HT-29 human colon cancer cells.[82] This cell-line-dependent variation is commonly related to differences in nanoparticle uptake efficiency, receptor expression, and endocytic mechanisms among cell types.

The reduced cytotoxicity of encapsulated EOs is also partly attributable to their slower, controlled release from nanocarriers. In this study, 48 hour incubation allowed partial evaluation of the sustained-release effects, although longer exposure times could further reveal the prolonged therapeutic potential of EO-NPs. Beyond controlled release, several additional factors likely contribute to the observed cytotoxic effects. The nano-encapsulation improves water dispersibility and solubility of the hydrophobic EO components, enhancing bioavailability at the cellular interface. Nanoparticle size and surface charge can influence cellular uptake, as smaller, positively charged chitosan-based nanoparticles are more efficiently internalized *via* endocytosis. Furthermore, coating with hyaluronic acid (HA) may facilitate receptor-mediated uptake through CD44 binding, enhancing selective delivery to cancer cells while minimizing toxicity to normal cells. The selectivity index, determined relative to RPE-1 cells, highlights the preferential cytotoxicity of EO-NPs toward cancer cells and supports the potential therapeutic safety of nano-encapsulation. The combination of sustained release, improved dispersion, enhanced solubility, and receptor-mediated internalization is likely to act synergistically to increase the cytotoxic efficiency of EO-NPs.

Overall, these findings highlight that nanoencapsulation not only modulates EO release kinetics but also affects multiple physicochemical and biological parameters that influence therapeutic outcomes. While nanoencapsulation can improve cytotoxic activity compared to free EOs, the extent of enhancement is system-specific and requires careful experimental evaluation for each formulation. Although ascorbic acid or other standard antioxidants may exhibit lower IC_{50} values, the EO-NPs system is designed as a multifunctional therapeutic material that combines cytotoxic activity, selectivity, and biocompatibility rather than replacing pure drugs or antioxidants. These results are consistent with previous studies demonstrating that nano-encapsulated bioactive compounds can induce cancer cell death more effectively than free counterparts while maintaining low toxicity and good biocompatibility.[83–86]

3.3.3 Gene expression and immunoblotting analyses. Samples were evaluated as anticancer agents on four cancerous and normal cells for their molecular activity in promoting apoptosis through both transcriptional and protein expression pathways. T Samples were evaluated as anticancer agents on four cancerous and normal cell lines for their molecular activity

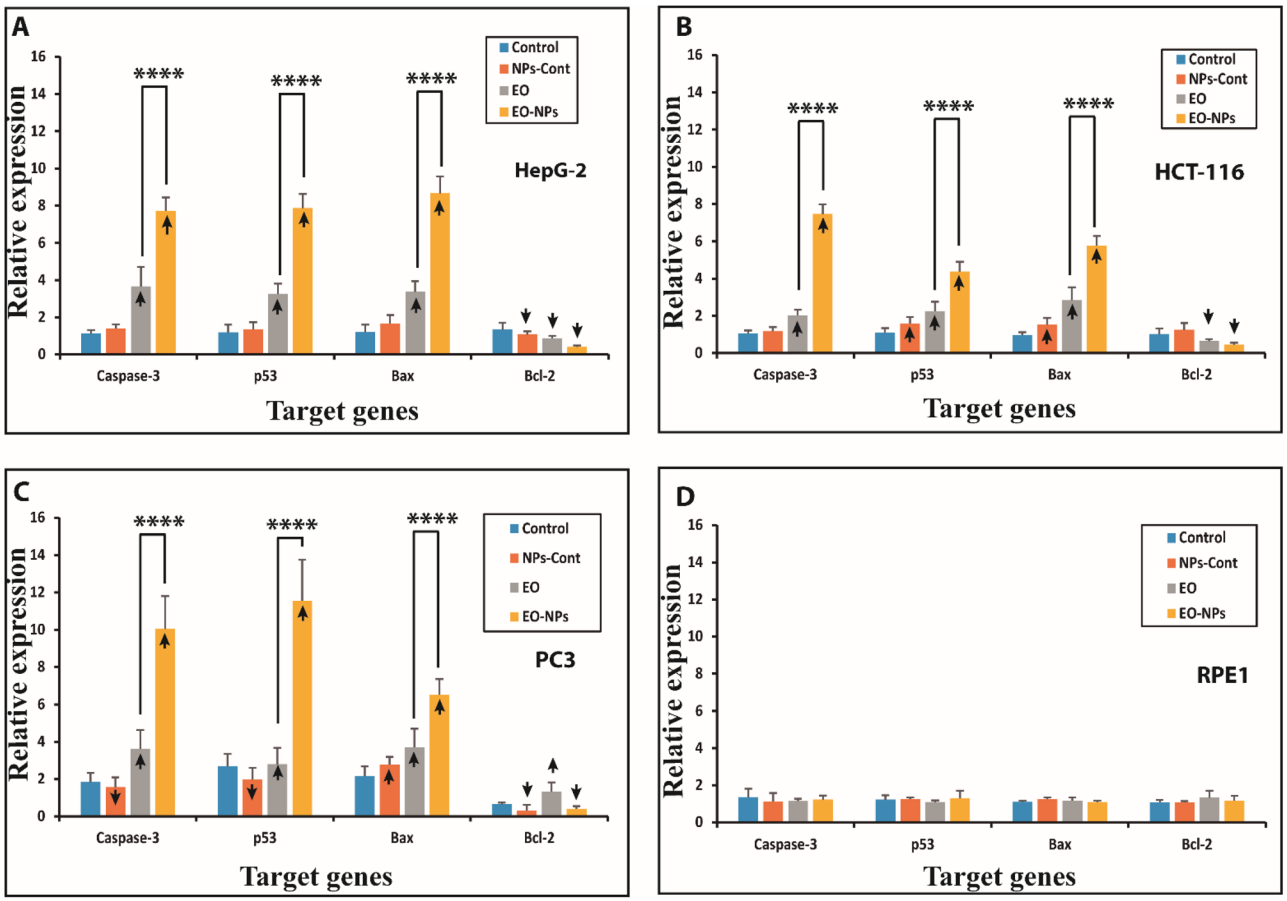

Fig. 5 Gene expression profiles of apoptotic markers in different cell lines after treatment with the prepared compounds. (A–D) Expression levels of key pro-apoptotic genes (p53, Bax, Caspase-3) and the anti-apoptotic gene (Bcl-2) are shown. Data are presented as mean ± standard deviation (SD) of three independent experiments performed in triplicate. Statistical analysis was conducted using two-way ANOVA followed by Tukey's multiple comparisons test. Significance thresholds are indicated as: *P < 0.05, **P < 0.01, ***P < 0.001, and ****P < 0.0001. Upward arrows (↑) indicate gene upregulation, while downward arrows (↓) indicate gene downregulation.

in promoting apoptosis through both transcriptional and protein expression pathways. The gene expression levels of pro- and anti-apoptotic genes were analyzed, including Caspase-3, p53, Bax, and Bcl-2 (Fig. 5).

The expression of pro-apoptotic genes (Caspase-3, p53, Bax) was significantly upregulated following treatment with EO-NPs at IC_{50} doses, whereas EO induced a lower transcriptional response. Conversely, the anti-apoptotic gene Bcl-2 was down-regulated in EO-NPs-treated cells, highlighting the shift toward apoptosis. Upregulation of Caspase-3 mRNA corresponds to activation of the intrinsic apoptotic pathway, where p53 induction increases Bax expression, leading to mitochondrial outer membrane permeabilization, cytochrome c release, and subsequent activation of caspases 9 and 3.[87] Functionally, the observed transcriptional changes translate into apoptosis execution: increased caspase activity, mitochondrial disruption, and inhibition of Bcl-2 facilitate programmed cell death.[88] In other words, these results indicate that nano-encapsulation of EO enhances apoptotic induction at both the transcriptional and functional levels. A plausible mechanism for the enhanced pro-apoptotic effects of EO-NPs involves hyaluronic acid surface functionalization. HA may mediate receptor (CD44)-dependent cellular uptake, increasing intracellular delivery of the nano-encapsulated EO and potentiating apoptosis in CD44-overexpressing cancer cells. Overall, the coordinated changes in pro- and anti-apoptotic markers correlate with observed apoptotic activity, supporting the conclusion that EO-NPs effectively promote programmed cell death in cancer cell lines while maintaining low cytotoxicity toward normal cells.[89,90]

3.3.4 Wound healing assay. EOs and plant-derived compounds are known for their promising pharmaceutical and cosmetic properties. In the current study, we assessed the wound healing potential of essential oil extracted from SG and its nanostructured form using the scratch assay on the BJ-1 normal human fibroblast cell line.

The results demonstrated that EO-NPs significantly enhanced fibroblast migration compared to the control and free EO, as evidenced by the marked reduction in wound gap over the assay period (Fig. 6).

This improvement in migration can be attributed to a combination of factors: (i) the bioactive properties of chitosan, which can stimulate fibroblast proliferation and migration; (ii)

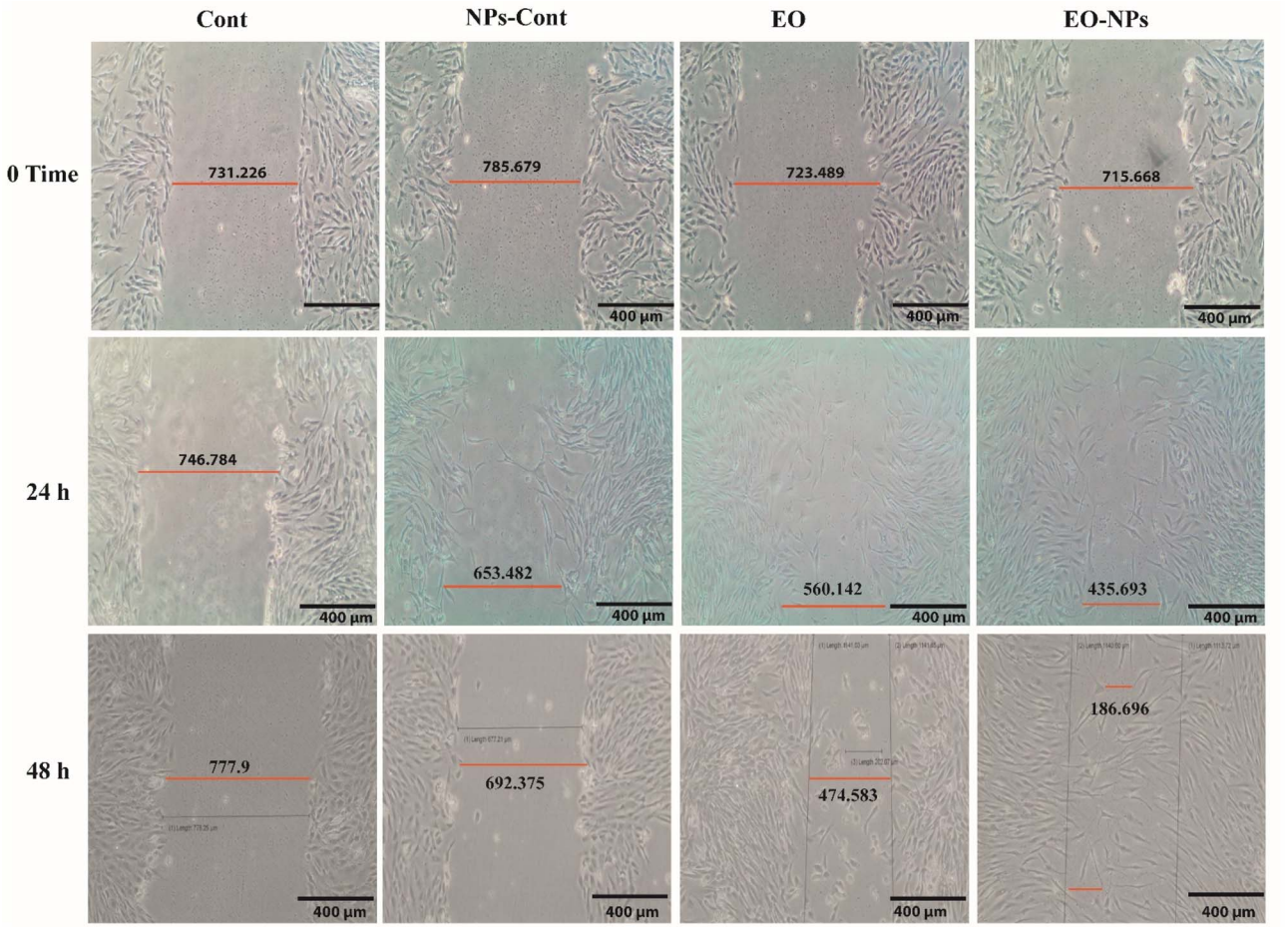

Fig. 6 Wound healing assay images showing the migration of cells treated with EO, EO-NPs, and their respective controls. Red lines indicate the wound closure distance, which was quantified using ImageJ software. The measured migration lengths are reported in µm.

hyaluronic acid signaling, which may engage CD44-mediated pathways that promote cytoskeletal reorganization and motility; and (iii) sustained, nanoscale delivery of essential oil-components, which maintains local EO concentration at the cell interface and protects labile bioactives from rapid volatilization or degradation. It is important to note that the scratch assay primarily reflects cell migration and does not fully recapitulate complete wound regeneration, which involves additional processes such as matrix remodeling, angiogenesis, and epithelialization. Nevertheless, these findings indicate that the nanostructured EO formulation can enhance the early phases of wound healing by promoting fibroblast migration more effectively than free EO.

Nanotechnology developments, including polysaccharide-based biopolymers such as chitosan and alginate, have been widely employed to improve wound dressings due to their biocompatibility, biodegradability, and capacity to accelerate tissue repair.[91,92] In particular, chitosan provides structural support and bioactivity for fibroblast migration, while HA functionalization enhances receptor-mediated interactions that may synergistically improve wound closure.[93–95]

Overall, the nanostructured EO formulation demonstrates superior migration-promoting effects compared to unmodified EO, highlighting the therapeutic potential of nanoscale delivery systems for accelerating wound closure and supporting tissue repair.

4 Conclusions

Chitosan–hyaluronic acid nano-encapsulations of *Senecio glaucus* essential oil were successfully prepared, demonstrating enhanced functional performance and bioactivity compared to the free oil. These results suggest that nano-encapsulation can enhance bioactivity; however, the findings primarily reflect *in vitro* outcomes, including antioxidant activity, cytotoxic effects, gene expression modulation, and fibroblast migration. Therefore, the potential applications of this nano-encapsulation should be considered prospective and exploratory, rather than as immediately translatable to broad biomedical or therapeutic use.

Dehydrofukinone, identified as the dominant component of the essential oil, likely contributes to the observed effects; however, the absence of performing a direct mechanistic analysis of individual constituents, the enhanced bioactivity should be interpreted as a result of the overall EO nano-encapsulation.

Future studies should focus on release profiling, oxidative and storage stability, and *in vivo* validation, in addition to investigating the specific contributions of dehydrofukinone and other key components to fully elucidate their mechanisms of action. This work provides a foundation for further optimization of EO nano-encapsulation for potential cosmetic or pharmaceutical applications.

Author contributions

Z. H. H. performed the conceptualization, methodology, investigation, data curation, formal analysis, visualization, and wrote the original draft. S. F. H. contributed to methodology, validation, formal analysis, supervision, and writing, review and editing. K. S. contributed to methodology, resources, supervision, and writing, review and editing. A. A. N. was responsible for conceptualization, supervision, project administration, funding acquisition, and writing, review and editing. H. S. M. S. contributed to conceptualization, methodology, supervision, and writing review and editing. All authors have read and approved the final manuscript.

Conflicts of interest

The authors assert that there are no conflicting interests, whether financial or otherwise, that could have influenced the research provided in this study.

Data availability

The datasets generated and/or analysed during this study are available from the corresponding author on reasonable request. Requests should be directed to amr.nassrallah@ejust.edu.eg.

Acknowledgements

The authors gratefully acknowledge the Egyptian Ministry of Higher Education for awarding a scholarship to pursue research at the Egypt–Japan University of Science and Technology.

References

1 A. Masyita, R. Mustika Sari, A. Dwi Astuti, B. Yasir, N. Rahma Rumata, T. B. Emran, F. Nainu and J. Simal-Gandara, Terpenes and terpenoids as main bioactive compounds of essential oils, their roles in human health and potential application as natural food preservatives, *Food Chem.:X*, 2022, **13**, 100217.

2 B. Yingngam, Chemistry of essential oils, in *Flavors and Fragrances in Food Processing: Preparation and Characterization Methods*, ed. A. M. Grumezescu and A. M. Holban, American Chemical Society, Washington, 2022, vol. 1433, pp. 189–223.

3 H. Falleh, M. Ben Jemaa, M. Saada and R. Ksouri, Essential oils: A promising eco-friendly food preservative, *Food Chem.*, 2020, **330**, 127268.

4 S. Burt, Essential oils: Their antibacterial properties and potential applications in foods—A review, *Int. J. Food Microbiol.*, 2004, **94**(3), 223–253.

5 S. Inouye, T. Takizawa and H. Yamaguchi, Antibacterial activity of essential oils and their major constituents against respiratory tract pathogens by gaseous contact, *J. Antimicrob. Chemother.*, 2001, **47**(5), 565–573.

6 J. K. R. da Silva, P. L. B. Figueiredo, K. G. Byler and W. N. Setzer, Essential oils as antiviral agents: Potential of essential oils to treat SARS-CoV-2 infection—An in silico investigation, *Int. J. Mol. Sci.*, 2020, **21**(10), 3426.

7 S. Đorđević, S. Petrović, S. Dobrić, M. Milenković, D. Vučićević, S. Žižić and J. Kukić, Antimicrobial, anti-inflammatory, anti-ulcer and antioxidant activities of Carlina acanthifolia root essential oil, *J. Ethnopharmacol.*, 2007, **109**(3), 458–463.

8 N. Mimica-Dukić, B. Božin, M. Soković, B. Mihajlović and M. Matavulj, Antimicrobial and antioxidant activities of three Mentha species essential oils, *Planta Med.*, 2003, **69**(5), 413–419.

9 G. L. Silva, C. Luft, A. Lunardelli, R. H. Amaral, D. A. Melo, M. V. Donadio, F. B. Nunes, M. S. Azambuja, J. C. Santana and C. Moraes, Antioxidant, analgesic and anti-inflammatory effects of lavender essential oil, *An. Acad. Bras. Cienc.*, 2015, **87**, 1397–1408.

10 M. B. Isman and C. M. Machial, Pesticides based on plant essential oils: From traditional practice to commercialization, *Adv. Phytomed.*, 2006, **3**, 29–44.

11 I. Jantan, W. O. Ping, S. D. Visuvalingam and N. W. Ahmad, Larvicidal activity of the essential oils and methanol extracts of Malaysian plants on Aedes aegypti, *Pharm. Biol.*, 2003, **41**(4), 234–236.

12 P. K. Mediratta, K. K. Sharma and S. Singh, Evaluation of immunomodulatory potential of Ocimum sanctum seed oil and its possible mechanism of action, *J. Ethnopharmacol.*, 2002, **80**(1), 15–20.

13 M. Abdollahi, H. Karimpour and H. R. Monsef-Esfehani, Antinociceptive effects of Teucrium polium L. total extract and essential oil in mouse writhing test, *Pharmacol. Res.*, 2003, **48**(1), 31–35.

14 A. Sharma, K. Gumber, A. Gohain, T. Bhatia, H. S. Sohal, V. Mutreja and G. Bhardwaj, Importance of essential oils and current trends in use of essential oils (aroma therapy, agrofood, and medicinal usage), in *Essential Oils*, ed. G. A. Nayik and M. J. Ansari, Academic Press, 2023, pp. 53–83.

15 J. Yammine, N. E. Chihib, A. Gharsallaoui, A. Ismail and L. Karam, Advances in essential oils encapsulation: Development, characterization and release mechanisms, *Polym. Bull.*, 2024, **81**(5), 3837–3882.

16 N. Lammari, O. Louaer, A. H. Meniai and A. Elaissari, Encapsulation of essential oils via nanoprecipitation process: Overview, progress, challenges and prospects, *Pharmaceutics*, 2020, **12**(5), 431.

17 W. Weisany, S. Yousefi, N. A.-R. Tahir, N. Golestanehzadeh, D. J. McClements, B. Adhikari and M. Ghasemlou, Targeted delivery and controlled release of essential oils using

nanoencapsulation: A review, *Adv. Colloid Interface Sci.*, 2022, **303**, 102655.
18 A. Nair, R. Mallya, V. Suvarna, T. A. Khan, M. Momin and A. Omri, Nanoparticles—Attractive carriers of antimicrobial essential oils, *Antibiotics*, 2022, **11**(1), 108.
19 Y. Zhu, C. Li, H. Cui and L. Lin, Encapsulation strategies to enhance the antibacterial properties of essential oils in food systems, *Food Control*, 2021, **123**, 107856.
20 M. Mondéjar-López, M. P. García-Simarro, P. Navarro-Simarro, L. Gómez-Gómez, O. Ahrazem and E. Niza, A review on the encapsulation of eco-friendly compounds in natural polymer-based nanoparticles as next generation nano-agrochemicals, *Int. J. Biol. Macromol.*, 2024, **280**, 136030.
21 D. Alemu, E. Getachew and A. K. Mondal, Study on the physicochemical properties of chitosan and their applications in the biomedical sector, *Int. J. Polym. Sci.*, 2023, **2023**, 5025341.
22 M. M. Khalafalla, H. M. Dafalla, A. Nassrallah, K. M. Aboul-Enein, H. A. El-Shemy and E. Abdellatef, Dedifferentiation of leaf explants and antileukemia activity of an ethanolic extract of cell cultures of Moringa oleifera, *Afr. J. Biotechnol.*, 2011, **10**(14), 2746–2750.
23 C. P. Fu, X. Y. Cai, S. L. Chen, H. W. Yu, Y. Fang, X. C. Feng, L. M. Zhang and C. Li, Hyaluronic acid-based nanocarriers for anticancer drug delivery, *Polymers*, 2023, **15**, 2317.
24 J. Alexander, The Mediterranean species of Senecio sections Senecio and Delphinifolius, *Notes R. Bot. Gard. Edinburgh*, 1979, **37**, 387–428.
25 H. De Pooter, L. De Buyck, N. Schamp, E. Aboutabl, A. De Bruyn and S. Husain, The volatile fraction of Senecio glaucus subsp. coronopifolius, *Flavour Fragrance J.*, 1986, **1**(4–5), 159–163.
26 T. Ramadan, A. Zaher, A. Amro and R. Sultan, Chemical composition and biological activity of capitula and shoots essential oils of Senecio glaucus L, *J. Essent. Oil Bear. Plants*, 2020, **23**(1), 168–183.
27 K. Basaid, R. Bouharroud, J. N. Furze, H. Benjlil, A. L. de Oliveira and B. Chebli, Biopesticidal value of Senecio glaucus subsp. coronopifolius essential oil against fungi, nematodes, and mites, *Mater. Today: Proc.*, 2020, **27**, 3082–3090.
28 H. Abdelaziz, Z. Salama and A. Nassrallah, S-limonene loaded gum Arabic nanoparticles ameliorates wound healing and inhibits herpes simplex virus, *Egypt. J. Chem.*, 2024, **67**(13), 2101–2106.
29 H. A. Ahmed, H. F. Aly, F. Abou-Elella, S. Salem, Z. Salama and A. M. Aboul-Enein, Investigation of nano-formulated bioactives on obese-induced rats, *Egypt. J. Chem.*, 2021, **64**(12), 7181–7193.
30 A. A. A. El-Maksoud, A. I. Makhlouf, A. B. Altemimi, I. H. A. El-Ghany, A. Nassrallah, F. Cacciola and T. G. Abedelmaksoud, Nano milk protein-mucilage complexes: Characterization and anticancer effect, *Molecules*, 2021, **26**(21), 6372.
31 Y. El-Amier, A. Abdelghany and A. A. Zaid, Green synthesis and antimicrobial activity of *Senecio glaucus*-mediated silver nanoparticles, *Res. J. Pharm., Biol. Chem. Sci.*, 2014, **5**(5), 631–642.
32 K. O. Fagbemi, D. A. Aina and O. O. Olajuyigbe, Soxhlet extraction versus hydrodistillation using the Clevenger apparatus: A comparative study on the extraction of a volatile compound from Tamarindus indica seeds, *Sci. World J.*, 2021, **2021**, 5961586.
33 Y. A. Hasanien, A. A. Nassrallah, A. G. Zaki and G. Abdelaziz, Optimization, purification, and structure elucidation of anthraquinone pigment derivative from Talaromyces purpureogenus as a novel antioxidant, anticancer, and kidney radio-imaging agent, *J. Biotechnol.*, 2022, **356**, 30–41.
34 S. A. Alsakhawy, H. H. Baghdadi, M. A. El-Shenawy and L. S. El-Hosseiny, Enhancement of lemongrass essential oil physicochemical properties and antibacterial activity by encapsulation in zein-caseinate nanocomposite, *Sci. Rep.*, 2024, **14**(1), 17278.
35 S. F. Tabatabaeain, E. Karimi and M. Hashemi, Satureja khuzistanica essential oil-loaded solid lipid nanoparticles modified with chitosan-folate: Evaluation of encapsulation efficiency, cytotoxic and pro-apoptotic properties, *Front. Chem.*, 2022, **10**, 904973.
36 H. A. Mohamed, A. A. Abdel-Shafi, H. Miyatake, M. E. El-Khouly and A. A. Nassrallah, Multifunctional N-substituted 2-pyridylbenzothiazole derivatives: singlet oxygen generation, protein binding, and photoactivated anticancer and antibacterial activities, *RSC Adv.*, 2025, **15**(52), 44649–44667.
37 E. Chiesa, R. Dorati, B. Conti, T. Modena, E. Cova, F. Meloni and I. Genta, Hyaluronic acid-decorated chitosan nanoparticles for CD44-targeted delivery of everolimus, *Int. J. Mol. Sci.*, 2018, **19**(8), 2310.
38 M. Vlcnovska, A. Stossova, M. Kuchynka, V. Dillingerova, H. Polanska, M. Masarik, R. Hrstka, V. Adam, V. Kanicky and T. Vaculovic, Comparison of metal nanoparticles (Au, Ag, Eu, Cd) used for immunoanalysis using LA-ICP-MS detection, *Molecules*, 2021, **26**(3), 630.
39 M. G. Abouelenein, A. A. El-Rashedy, H. M. Awad, A. F. El Farargy, I. F. Nassar and A. Nassrallah, Synthesis, molecular modeling insights, and anticancer assessment of novel polyfunctionalized pyridine congeners, *Bioorg. Chem.*, 2023, **141**, 106910.
40 R. Li, J. Li, T. M. Y. Cheung, B. S. Y. Ho and G. P. H. Leung, Comparison of the major chemical constituents and antioxidant effects in Amauroderma rugosum and Ganoderma lucidum, *Biomed. Transl. Sci.*, 2020, **1**(1), 1–6.
41 R. Re, N. Pellegrini, A. Proteggente, A. Pannala, M. Yang and C. Rice-Evans, Antioxidant activity applying an improved ABTS radical cation decolorization assay, *Free Radicals Biol. Med.*, 1999, **26**(9), 1231–1237.
42 C. C. Liang, A. Y. Park and J. L. Guan, In vitro scratch assay: A convenient and inexpensive method for analysis of cell migration in vitro, *Nat. Protoc.*, 2007, **2**(2), 329–333.
43 M. Fronza, B. Heinzmann, M. Hamburger, S. Laufer and I. Merfort, Determination of the wound healing effect of Calendula extracts using the scratch assay with 3T3 fibroblasts, *J. Ethnopharmacol.*, 2009, **126**(3), 463–467.

44 E. Lizarraga, E. Romano, A. B. Raschi, P. Leyton, C. Paipa, C. A. Catalán and S. A. Brandán, A structural and vibrational study of dehydrofukinone combining FTIR, FT-Raman, UV–visible and NMR spectroscopies with DFT calculations, *J. Mol. Struct.*, 2013, **1048**, 331–338.

45 R. J. Nachman, Tetrahydroligularenolide and related eremophilanes from Senecio aureus, *Phytochemistry*, 1983, **22**(3), 780–782.

46 A. M. Rodríguez, S. Montanaro, A. Bardon, E. Cartagena and S. Borkosky, A Puna collection of Senecio punae, main source of a versatile eremophilane-type ketone, *Nat. Prod. Commun.*, 2016, **11**(8), 1061–1064.

47 M. C. Verni, J. A. Garay, L. Mendoza, A. Bardón, S. Borkosky, M. E. Arena and E. Cartagena, Lipophilic 9,10-dehydrofukinone action on pathogenic and non-pathogenic bacterial biofilms, *Chem. Biodiversity*, 2020, **17**(6), e1900507.

48 F. Bohlmann, W. Kramp, H. Robinson and R. M. King, A norsesquiterpene from Senecio humillimus, *Phytochemistry*, 1981, **20**(7), 1739–1740.

49 M. M. Elghonemy, A. F. Essa, A. F. Osman, D. D. Khalaf, A. E. G. El-Gendy, A. M. Abd-ElGawad, A. Umeyama and A. I. Elshamy, Profiling key aroma compounds of Senecio glaucus L. and their antimicrobial and antioxidant activities, *Chem. Biodiversity*, 2024, **21**(5), e202302112.

50 J. K. A. Xavier, N. S. F. Alves, W. N. Setzer and J. K. R. da Silva, Chemical diversity and biological activities of essential oils from Licaria, Nectandra and Ocotea species, *Biomolecules*, 2020, **10**(6), 869.

51 Q. Garlet, L. C. Pires, D. Silva, S. Spall, L. Gressler, M. Bürger, B. Baldisserotto and B. Heinzmann, Effect of (+)-dehydrofukinone on GABAA receptors and stress response in fish model, *Braz. J. Med. Biol. Res.*, 2015, **49**(1), e4872.

52 Q. I. Garlet, L. da Costa Pires, L. H. Milanesi, J. R. Marafiga, B. Baldisserotto, C. F. Mello and B. M. Heinzmann, (+)-Dehydrofukinone modulates membrane potential and delays seizure onset by GABAA receptor-mediated mechanism in mice, *Toxicol. Appl. Pharmacol.*, 2017, **332**, 52–63.

53 M. T. Islam, E. S. Ali, S. J. Uddin, S. Shaw, M. A. Islam, M. I. Ahmed, M. C. Shill, U. K. Karmakar, N. S. Yarla and I. N. Khan, Phytol: A review of biomedical activities, *Food Chem. Toxicol.*, 2018, **121**, 82–94.

54 L. L. Zhang, Y. Chen, Z. J. Li, G. Fan and X. Li, Production, function, and applications of the sesquiterpenes valencene and nootkatone, *J. Agric. Food Chem.*, 2022, **71**(1), 121–142.

55 Y. V. Gyrdymova and S. A. Rubtsova, Caryophyllene and caryophyllene oxide: A variety of chemical transformations and biological activities, *Chem. Pap.*, 2022, **76**, 1–39.

56 G. M. de Lacerda Leite, M. de Oliveira Barbosa, M. J. P. Lopes, G. de Araújo Delmondes, D. S. Bezerra, I. M. Araújo, C. D. C. de Alencar, H. D. M. Coutinho, L. R. Peixoto and J. M. Barbosa-Filho, Pharmacological and toxicological activities of α-humulene and its isomers: A systematic review, *Trends Food Sci. Technol.*, 2021, **115**, 255–274.

57 M. Glumac, Z. Jažo, V. Paštar, A. Golemac, V. Čikeš Čulić, S. Bektić, M. Radan and I. Carev, Chemical profiling and bioactivity assessment of Helichrysum italicum essential oil, *Molecules*, 2023, **28**(14), 5299.

58 C. Khaleel, N. Tabanca and G. Buchbauer, α-Terpineol, a natural monoterpene: A review of its biological properties, *Open Chem.*, 2018, **16**(1), 349–361.

59 R. P. Adams, *Identification of Essential Oil Components by Gas Chromatography/mass Spectrometry*, Allured Publishing Corporation, Carol Stream (IL), 4th edn, 2017.

60 V. I. Babushok, P. J. Linstrom and I. G. Zenkevich, Retention indices for frequently reported compounds of plant essential oils, *J. Phys. Chem. Ref. Data*, 2011, **40**(4), 1–46.

61 H. A. Ahmed, A. Abdel-Fattah, Z. A. Salama and A. E. Abd El-Wahab, Evaluation of antimicrobial potential of free gallic acid and its polyvinyl-based nano-formulation, *Sci. Rep.*, 2025, **15**(1), 34281.

62 H. A. Ahmed, Y. A. El-Maradny, M. A. Shalaby, H. El-Menshawy and A. E. Abd EL-Wahab, Isolation and characterization of chitosan from shrimp shell waste and preparation of salicylic acid-loaded chitosan nanoparticles, *Sci. Rep.*, 2025, **15**(1), 19263.

63 A. A. Goda, M. F. El-ssayad, H. A. Ahmed, E. G. Ayad, H. Effat and S. H. Salem, Evaluation of antimicrobial, antioxidant and anticancer activity of Teucrium polium extracts and application of its nanoparticles as food preservative, *Discover Food*, 2025, 1–19.

64 X. Chen, S. Shang, F. Yan, H. Jiang, G. Zhao, S. Tian, R. Chen, D. Chen and Y. Dang, Antioxidant activities of essential oils and their major components in scavenging free radicals and reducing oxidative stress, *Molecules*, 2023, **28**(11), 4559.

65 R. Mazrou, E. F. Ali, S. Hassan and F. A. S. Hassan, Role of chitosan nanoparticles in enhancing essential oil productivity and antioxidant capacity in Matricaria chamomilla L, *Horticulturae*, 2021, **7**(12), 574.

66 S. Noori, F. Zeynali and H. Almasi, Antimicrobial and antioxidant efficiency of nanoemulsion-based edible coating containing ginger essential oil on chicken breast fillets, *Food Control*, 2018, **84**, 312–320.

67 D. C. Jung, S. Y. Lee, J. H. Yoon, K. P. Hong, Y. S. Kang, S. R. Park, S. K. Park, S. D. Ha, G. H. Kim and D. H. Bae, Inhibition of pork and fish oxidation by plastic film coated with horseradish extract, *LWT–Food Sci. Technol.*, 2009, **42**(4), 856–861.

68 P. Homayonpour, H. Jalali, N. Shariatifar and M. Amanlou, Effects of nano-chitosan coatings incorporating free and nano-encapsulated cumin essential oil on sardine fillet quality, *Int. J. Food Microbiol.*, 2021, **341**, 109047.

69 M. Abdollahzadeh, A. H. Elhamirad, N. Shariatifar, M. Saeidiasl and M. Armin, Effects of nano-chitosan coatings incorporating essential oil of Heracleum persicum on rainbow trout quality, *Int. J. Food Microbiol.*, 2023, **385**, 109996.

70 Y. Han, J. Cao, M. Li, P. Ding, Y. Yang, O. V. Okoro, Y. Sun, G. Jiang, A. Shavandi and L. Nie, Fabrication of multifunctional hydrogel dressings using modified

hyaluronic acid and chitosan, *Front. Chem.*, 2024, **12**, 1402870.

71 S. Manivannan and S. Narayan, Polyethylene glycol crosslinked chitosan nanoparticles for co-delivery of docetaxel and 5-fluorouracil, *Macromol. Res.*, 2024, **32**(4), 371–392.

72 N. S. Chatterjee, P. K. Dara, S. Perumcherry Raman, D. K. Vijayan, J. Sadasivam, S. Mathew, C. N. Ravishankar and R. Anandan, Nanoencapsulation improves in vivo antioxidant potential of black carrot anthocyanin, *J. Sci. Food Agric.*, 2021, **101**(12), 5264–5271.

73 H. H. Elbehery, H. A. Ahmed, S. Sayed Ibrahim, W. Abouamer and A. Farouk, Gum Arabic containing Allium sativum essential oil-based nanoparticles as grain protectant, *PLoS One*, 2025, **20**(10), e0334926.

74 H. Elmotasem, A. A. Salama and E. S. Shalaby, Hyaluronate functionalized nanovesicular system of ferulic acid targeting diabetic nephropathy, *Int. J. Biol. Macromol.*, 2024, **279**, 135292.

75 F. Della Sala, G. Longobardo, A. Fabozzi, M. di Gennaro and A. Borzacchiello, Hyaluronic acid-based wound dressing with antimicrobial properties, *Appl. Sci.*, 2022, **12**(6), 3091.

76 P. Makvandi, C. Caccavale, F. Della Sala, S. Zeppetelli, R. Veneziano and A. Borzacchiello, Natural formulations as antioxidant complement to hyaluronic acid-based topical applications, *Polymers*, 2020, **12**(8), 1847.

77 M. R. Hajizadeh, H. Maleki, M. Barani, M. A. Fahmidehkar, M. Mahmoodi and M. Torkzadeh-Mahani, Cytotoxicity assay of D-limonene niosomes as nano-carrier, *Res. Pharm. Sci.*, 2019, **14**(5), 448–458.

78 A. M. Hamed, A. A. Abd El-Maksoud, M. A. Hassan, E. Tsakali, J. F. Van Impe, H. A. Ahmed and A. A. Nassrallah, Enhancing functional buffalo yogurt using essential oils, *J. Dairy Sci.*, 2024, **107**(9), 6437–6450.

79 E. M. Awadalla, M. Elkady, A. Badr and A. A. Nassrallah, Green engineering of potato starch–polyurethane biofilters for oil–water recovery, *J. Water Process Eng.*, 2026, **85**, 109828.

80 V. S. Periasamy, J. Athinarayanan and A. A. Alshatwi, Anticancer activity of nanoemulsion formulation of Nigella sativa essential oil, *Ultrason. Sonochem.*, 2016, **31**, 449–455.

81 W. A. Al-Otaibi, M. H. Alkhatib and A. N. Wali, Cytotoxicity enhancement in cancer cells using essential oils in nanoemulsions, *Biomed. Pharmacother.*, 2018, **106**, 946–955.

82 F. Salehi, T. Jamali, G. Kavoosi, S. K. Ardestani and S. N. Vahdati, Stabilization of Zataria essential oil with nanoemulsion for enhanced cytotoxicity, *Int. J. Biol. Macromol.*, 2020, **164**, 3645–3655.

83 O. A. A. Alabrahim, J. M. Lababidi, W. Fritzsche and H. M. E. S. Azzazy, Essential oil loaded nanocarriers in cancer treatment, *Nanoscale Adv.*, 2024, **6**(22), 5511–5562.

84 B. A. Samling, Z. Assim, W. Y. Tong, C. R. Leong, S. A. Rashid, N. N. S. N. M. Kamal, M. Muhamad and W. N. Tan, Cynometra cauliflora essential oils loaded-chitosan nanoparticles: evaluations of their antioxidant, antimicrobial and cytotoxic activities, *Int. J. Biol. Macromol.*, 2022, **210**, 742–751.

85 H. A. Ahmed, A. A. Nassrallah, M. A. Abdel-Raheem and H. H. Elbehery, Lemon peel essential oil nano-formulation to control Agrotis ipsilon, *Sci. Rep.*, 2023, **13**(1), 17922.

86 N. H. Elghazawy, A. Hefnawy, N. K. Sedky, I. M. El-Sherbiny and R. K. Arafa, Nanoformulation of quinolone scaffold-based anticancer agents, *Eur. J. Pharm. Sci.*, 2017, **105**, 203–211.

87 Q. Gu, J. Z. Xing, M. Huang, X. Zhang and J. Chen, Nanoformulation of paclitaxel to enhance cancer therapy, *J. Biomater. Appl.*, 2013, **28**(2), 298–307.

88 P. Panyajai, N. Viriyaadhammaa, S. Tima, S. Chiampanichayakul, P. Dejkriengkraikul, S. Okonogi and S. Anuchapreeda, Anticancer activity of Curcuma aeruginosa essential oil nano-formulations, *BMC Complementary Med. Ther.*, 2024, **24**(1), 16.

89 K. AbouAitah and W. Lojkowski, Nanomedicine to enhance application of essential oils in cancer, *Pharmaceuticals*, 2022, **15**(7), 793.

90 K. AbouAitah, A. Nassrallah, A. A. Soliman, A. Swiderska-Sroda, T. Chudoba, J. Smalc-Koziorowska and W. Lojkowski, Mesoporous silica nanoparticles loaded with ellagic acid for colon cancer, *Nanomaterials*, 2025, **15**(20), 1547.

91 I. A. Soliman, Y. A. Hasanien, A. G. Zaki, H. A. Shawky and A. A. Nassrallah, Irradiation impact on anthraquinone pigment and its application as food preservative, *BMC Microbiol.*, 2022, **22**(1), 325.

92 F. Farmani, M. Moein, A. Amanzadeh, H. M. Kandelous, Z. Ehsanpour and M. Salimi, Antiproliferative evaluation of Ziziphus spina-christi leaf extracts in MCF-7 cells, *Asian Pac. J. Cancer Prev.*, 2016, **17**(1), 315–321.

93 H. M. Abo-Salem, A. Nassrallah, A. A. Soliman, M. S. Ebied, M. E. Elawady, S. A. Abdelhamid, E. R. El-Sawy, Y. A. Al-Sheikh and M. A. Aboul-Soud, Synthesis and bioactivity of spiro pyrazole-oxindole congeners, *Molecules*, 2020, **25**(5), 1124.

94 E. Sienkiewicz-Szłapka, B. Jarmołowska, S. Krawczuk, E. Kostyra, H. Kostyra and K. Bielikowicz, Transport of bovine milk-derived opioid peptides across Caco-2 monolayer, *Int. Dairy J.*, 2009, **19**(4), 252–257.

95 K. AbouAitah, A. A. Soliman, A. Swiderska-Sroda, A. Nassrallah, J. Smalc-Koziorowska, S. Gierlotka and W. Lojkowski, Co-delivery system of curcumin and colchicine using mesoporous silica nanoparticles, *Pharmaceutics*, 2022, **14**(12), 2770.